LIQUID CIRCULATION, GAS HOLDUP AND PRESSURE DROP IN BUBBLE COLUMN WITH DRAUGHT TUBE

Kozo KOIDE, Shinji IWAMOTO, Yukitoshi TAKASAKA,
Shinji MATSUURA, Etsuo TAKAHASHI
and Motohiko KIMURA
Department of Chemical Engineering, Shizuoka University, Hamamatsu 432

Hiroshi KUBOTA
Research Laboratory of Resources Utilization,
Tokyo Institute of Technology, Yokohama 227

The effects of gas velocity and geometrical dimensions of apparatus on the flow rate Q_L of circulating liquid, gas holdups and pressure drops in bubble columns with draught tube were examined. It was found that Q_L increases with increasing gas velocity, column diameter, draught tube length, and height of the lower end of draught tube, and decreases with increasing liquid viscosity. It was also found that the maximum value of Q_L is observed for constant values of gas velocity and column diameter, when the diameter ratio of draught tube and column is about 0.6.

Empirical equations for gas holdups in draught tube and annulus and the pressure drops due to flow reversals, necessary for estimating Q_L, are proposed.

Introduction

The bubble column with draught tube is widely used in various processes,[2] including chemical, fermentation, leaching and waste water treatment processes. Gas is bubbled into a draught tube, and the liquid flows upwards in the tube and downwards in the annulus by air-lift action.

Many studies[4,6-8,11] of this circulating liquid flow have been made, but the results of flow rate estimation of circulating liquid proposed in these studies do not agree with each other. This disagreement might be due to the difference of experimental techniques used for measuring liquid flow rate or inadequate assumptions used in deriving the equation for estimating liquid flow rates.

The purpose of this work is to observe experimentally the effects of gas velocity U_G and geometrical dimensions of apparatus on the flow rate of circulating liquid and to established a method of estimating the flow rate in a bubble column with draught tube into which gas is dispersed.

1. Fundamentals

Figure 1 shows a scheme of the bubble column with draught tube.

Macroscopic mass, momentum and energy bal-

ances in the column give inherent relationships among the flow rate of circulating liquid, liquid velocities, gas holdups and reversal losses due to reversing flow direction. A mass balance between section 1–4 in Fig. 1 gives

$$Q_L = S_a \bar{U}_{La} = S_i \bar{U}_{Li} = S_o \bar{U}_{Lc}/2 \qquad (1)$$

where

$$S_a = \pi \{D_o^2 - (D_i + 2t_w)^2\}/4, \qquad S_i = \pi D_i^2/4$$

and

$$S_o = \pi D_o^2/4.$$

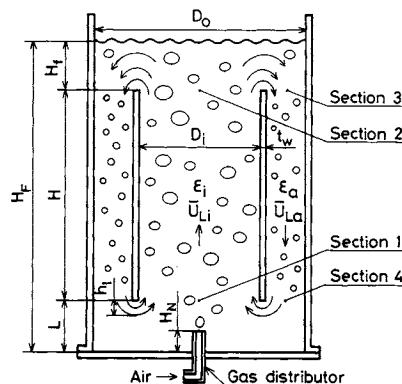Momentum and energy balances among sections 1–4 in Fig. 1 give the following equations for $H_N \leqq L$.

Fig. 1. Scheme of bubble column with draught tube and with gas dispersion into it.

$$P_1 - P_2 = (4H\tau_{wi}/D_i) + \rho_L gH(1 - \varepsilon_i) \qquad (2)$$

$$P_2 - P_3 = \Delta P_u + \frac{\rho_L}{2}\left[\left(\frac{\bar{U}_{La}}{1-\varepsilon_a}\right)^2 - \left(\frac{\bar{U}_{Li}}{1-\varepsilon_i}\right)^2\right] \qquad (3)$$

$$P_3 - P_4 = (4H\tau_{wa}/D_e) - \rho_L gH(1 - \varepsilon_a) \qquad (4)$$

$$P_4 - P_1 = \Delta P_l + \frac{\rho_L}{2}\left[\left(\frac{\bar{U}_{Li}}{1-\varepsilon_i}\right)^2 - \left(\frac{\bar{U}_{La}}{1-\varepsilon_a}\right)^2\right] \qquad (5)$$

Adding Eqs. (2)–(5) gives

$$\rho_L gH(\varepsilon_i - \varepsilon_a) = \Delta P_l + \Delta P_u + \Delta P_{fa} + \Delta P_{fi} \qquad (6)$$

where

$$\Delta P_{fa} = 4H\tau_{wa}/D_e \qquad (7)$$

$$\Delta P_{fi} = 4H\tau_{wi}/D_i \qquad (8)$$

For $H_N > L$ in Fig. 1, the equation corresponding to Eq. (6) is given by Eq. (9).

$$\rho_L g\varepsilon_i(H + L - H_N) - \rho_L gH\varepsilon_a$$
$$= \Delta P_l + \Delta P_u + \Delta P_{fa} + \Delta P_{fi} \qquad (9)$$

where

$$\Delta P_{fi} = \frac{4\tau_{w0}(H_N - L)}{D_i} + \frac{4\tau_{wi}(H + L - H_N)}{D_i} \qquad (10)$$

Single-phase liquid flow is assumed in the region of $L \leq y \leq H_N$ as indicated in the first term of the right side of Eq. (10), though bubbles are entrained from the annulus by liquid flow and exist in this region.

ε_a, ε_i, ΔP_l, ΔP_u, ΔP_{fa} and ΔP_{fi} in Eqs. (6) and (9) must be given as functions of average gas velocity $\bar{U}_G$, Q_L, the properties of the liquid and the geometrical dimensions of the column so that Q_L, which is related to $\bar{U}_{Li}$ and $\bar{U}_{La}$ through Eq. (1), can be estimated by Eq. (6) or Eq. (9).

2. Experimental

2.1 Experimental apparatus and conditions

The experimental apparatus used in this work is shown in Fig. 2. Three of kinds of plexiglass columns with flat bottom were used. Their dimensions are 0.1 m dia., 1 m in height, 0.14 m dia., 1 m and 2 m in height, and 0.30 m dia., 2 m in height. Table 1 shows the dimensions of draught tubes and their height from the base plate of the column. Single orifice plates, single nozzles and perforated plates were used as gas distributors, details of which are shown in Table 2. The gas velocity $\bar{U}_G$ of air used was 0.00192–0.128 m·s^{-1}.

The liquids used were 10 mol·m^{-3} KCl aqueous solution and 100 mol·m^{-3} KCl–50 wt% glycerol aqueous solution at a temperature of 293.2 K. The height of liquid without gas flowing was kept at 0.741–1.55 m above the base plate of the column. During a run, the liquid was neither fed nor dis-
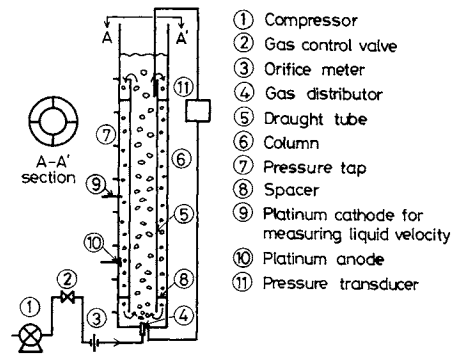
charged. Table 3 shows the properties of the liquid at operating temperature.

2.2 Measurement of liquid flow rate

The flow rate of circulating liquid was obtained by measuring the liquid velocities U_{La} in the annulus. U_{La} was obtained by measuring diffusion current i_d of dissolved oxygen on a fine spherical platinum cathode. In this work potassium chloride was used as a supporting electrolyte, and in this case the following reaction occurs on the platinum cathode:
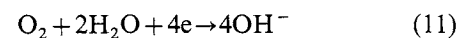
$$O_2 + 2H_2O + 4e \rightarrow 4OH^- \qquad (11)$$

Figure 3 shows details of the platinum cathode, which is insulated electrically excepts for its spherical

Fig. 2. Experimental apparatus.

① Compressor
② Gas control valve
③ Orifice meter
④ Gas distributor
⑤ Draught tube
⑥ Column
⑦ Pressure tap
⑧ Spacer
⑨ Platinum cathode for measuring liquid velocity
⑩ Platinum anode
⑪ Pressure transducer

Table 1. Experimental apparatus

D_o [m]	D_i [m]	t_w [mm]	H [m]	L/D_i [—]	H_L [m]	Gas distributors*
0.100	0.052	3	0.70	0.50	0.84	S1
0.100	0.066	3	0.70	0.50	0.84	S1
0.140	0.066	3	0.70	0.50	0.84	S2, S3, P1, P2
0.140	0.078	5	0.70	0.50	0.84	S2
0.140	0.082	3	0.70	0.24–1.0	0.74–0.94	S2, S3, P1
0.140	0.082	3	0.70	0.24–1.0	0.74–0.94	P2, N1, N2
0.140	0.082	3	1.40	0.50	1.54	S2, S3
0.140	0.082	2	0.70	0.50	0.84	S2, S3
0.140	0.094	3	0.70	0.50	0.84	S3
0.140	0.104	3	0.70	0.50	0.84	S3
0.300	0.190	5	1.40	0.50	1.55	N3

* Details are shown in Table 2.

Table 2. Details of gas distributors

Key	Gas distributor	δ [mm]	N [—]	H_N [m]
S1	Single orifice plate	2.2	1	0
S2	Single orifice plate	3.0	1	0
S3	Single orifice plate	3.6	1	0
N1	Single nozzle	4.0	1	0.041
N2	Single nozzle	4.0	1	0.216
N3	Single nozzle	15.0	1	0
P1	Perforated plate	0.5	19	0
P2	Perforated plate	1	7	0

Table 3. Properties of liquids

Liquid	ρ_L [kg·m^{-3}]	$\mu_L \times 10^3$ [Pa·s]	$\sigma_L \times 10^3$ [N·m^{-1}]
10 mol·m^{-3} KCl aq. soln.	998.2	1.01	72.6
100 mol·m^{-3} KCl −50 wt% Glycerol aq. soln.	1134	6.09	68.0
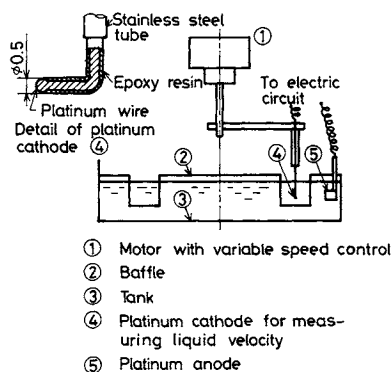
Fig. 3. Experimental apparatus of calibrating platinum cathode for measuring liquid velocity.

Fig. 4. Diffusion current vs. probe velocity.

tip and is supported with a stainless steel tube 2 mm in diameter. An experimental equipment for calibrating the relation of i_d vs. liquid velocity on this spherical electrode is also shown in Fig. 3. After the liquid in the tank (3 in Fig. 3) was saturated with air, the spherical electrode installed on an arm fitted to a motor was rotated at a constant speed in the liquid, and a certain voltage where a diffusion current i_d was observed was applied between the spherical cathode and the platinum anode shown in Fig. 3. A time-averaged value of i_d was obtained by converting the output analog signals from an electric circuit including the spherical cathode into digital signals at a sampling rate of 500 s^{-1} for 40–80 s and calculating an average value of these signals with a digital computer. **Figure 4** shows a calibrated relation of i_d vs. U_p for the spherical cathode.

To measure the flow rate of circulating liquid in the column, the spherical cathode was installed on the radially moving device fitted to the column, and the voltage necessary to measure i_d was applied between the spherical cathode and an anode of platinum foil fixed on the inside wall of the column. The output signals from the electric circuit were sampled at a rate of 500 s^{-1} for 80 s, and converted to the liquid velocities by the relation given in Fig. 4. These velocities were averaged to give U_{La}. In the annulus small bubbles of sizes below 4 mm were observed, and when these bubbles rapped the spherical cathode the values of the output signals dropped sharply. These signals were excluded from the data used to evaluate
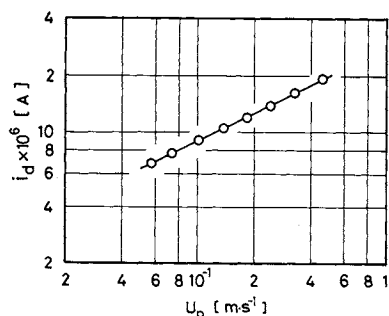
U_{La}. U_{La} obtained at six measuring points in radial direction of the annulus were multiplied by $(1 - \varepsilon_a)$ and used to evaluate Q_L by graphical integration.

2.3 Gas holdup and reversal losses

Axial distributions of static pressures in the draught tube and the annulus were measured: in the annulus the static pressure differences between pressure taps installed on the column wall were measured, and in the draught tube the static pressure difference between a reference pressure tap in the base plate and a 2 mm Prandtl tube inserted in the draught tube. Gas holdups and reversal losses were found from Eqs. (2)–(5) with the measured static pressure distributions, τ_{wi} and τ_{wa}, where τ_{wi} and τ_{wa} were calculated by using Takamatsu's results[15] and the friction factor for single-phase liquid flow,[5] respectively.

3. Results and Discussion

3.1 Static pressure distribution and reversal losses

Figure 5 shows ΔP_t, the static pressure difference detected by a pressure transducer, two conduits of which were connected to the pressure tap of the base plate of the column and to an arbitrary pressure tap of the column or the Prandtl tube inserted into the draught tube. The static pressure P at a position whose height from the base plate is y is related to ΔP_t by Eq. (12).

$$\Delta P_t = (P + \rho_L g y) - P_B \tag{12}$$

where P_B is the static pressure at the base plate of the column. An approximately linear relationship exists between ΔP_t and y except for the lower part of the draught tube, where the entering fluid contracts and shows a lower value of ΔP_t than that expected in the case without contraction. Therefore, to obtain the static pressure difference $(P_4 - P_1)$ in Eq. (5) without the effect of contraction, the section of the straight-line plot of ΔP_t vs. y is extrapolated to the lower end of the draught tube as shown in Fig. 5. The reversal loss at the lower end of the draught tube, ΔP_l, was calculated from the measured value of $(P_4 - P_1)$ and Eq. (5).
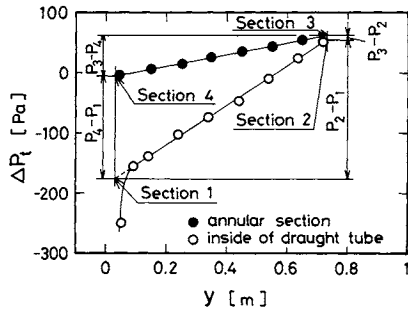
Fig. 5. ΔP_t vs. y.

Figure 6 shows that ΔP_l increases with increase in $\bar{U}_{La}/(1-\varepsilon_a)$, and the column of $D_i = 0.082$ m gives relatively low values of ΔP_l compared to those observed in columns having D_i other than 0.082 m.

Figure 7 shows that when the distance L between the lower end of the draught tube and the base plate of the column is increased from 2 cm to 4.2 cm ($L/D_i = 0.24$–0.5 in the column of $D_o = 0.14$ m and $D_i = 0.082$ m), ΔP_l decreases drastically, but further increase in L has no effect on ΔP_l. This dependence of ΔP_l on L is similar to the results given by Blenke et al.[3] for single-phase liquid flow. Figure 7 also shows that with the same column dimensions and the same liquid velocity, the more viscous liquid gives larger value of ΔP_l, and the effect of D_o on ΔP_l is small if D_i/D_o and L/D_i are kept constant.

The liquid flow under the draught tube is visualized by the paths of tiny bubbles entrained by the liquid flow from the annulus into the draught tube. This observation shows that the liquid flow from the annulus converges drastically under the lower end of the draught tube with change in its flow direction and then diverges into the draught tube. Therefore, ΔP_l is assumed to be expressed in the form of loss due to the convergence-divergence flow model where the effect of flow reversal on ΔP_l is included in an effective width h_l of the gas-liquid flow path under the lower end of the draught tube shown in Fig. 1.

$$\Delta P_l = 0.45 \left[\frac{\rho_L}{2} \left\{ \frac{S_a \bar{U}_{La}}{\pi D_1 h_l (1 - \varepsilon_a)} \right\}^2 \right] \left(1 - \frac{\pi D_1 h_l}{S_a} \right)$$

$$+ \frac{\rho_L}{2} \left(\frac{\bar{U}_{Li}}{1 - \varepsilon_i} \right)^2 \left\{ \frac{S_i (1 - \varepsilon_i)}{\pi D_1 h_l (1 - \varepsilon_a)} - 1 \right\}^2 \quad (13)$$

where $(\pi D_1 h_l)$ is the minimum cross-sectional area of gas-liquid flow under the lower end of the draught tube. h_l was evaluated by Eq. (13) using measured values of ΔP_l, $\bar{U}_{Li}$, $\bar{U}_{La}$, ε_i and ε_a, and was correlated with column dimensions, flow conditions and liquid properties for columns of $(L/D_i) \leq 0.5$.

$$\frac{h_l}{D_o} = 0.187(1 - \varepsilon_a)^{-0.310} \left(\frac{\bar{U}_{Li}}{\sqrt{gD_i}} \right)^{0.310} \left(\frac{L}{D_i} \right)^{0.405}$$
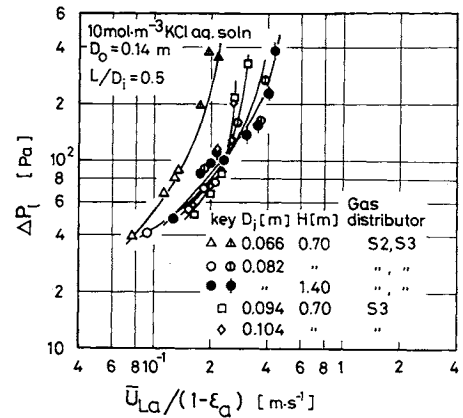

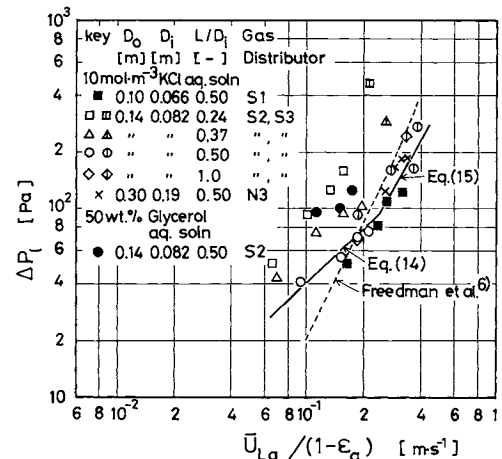**Fig. 6.** Effect of $\bar{U}_{La}/(1-\varepsilon_a)$ and D_i on ΔP_l.

Fig. 7. Effect of $\bar{U}_{La}/(1-\varepsilon_a)$, μ_L, L and column diameter on ΔP_l (Lines: estimated for air–10 mol·m^{-3} KCl aq. soln system in column of $D_o = 0.14$ m, $D_i = 0.082$ m and $L/D_i = 0.50$).

$$\times \left(\frac{S_a}{S_o} \right)^{0.778} \left(\frac{S_i}{S_o} \right)^{0.176} \left(\frac{g\mu_L^4}{\rho_L \sigma_L^3} \right)^{-0.0218} \quad (14)$$

$$\text{for} \quad 0.710 \leq \phi \leq 1$$

$$\frac{h_l}{D_o} = 1.05 \left(\frac{L}{D_i} \right)^{0.724} \left(\frac{S_a}{S_o} \right)^{2.28} \left(\frac{S_i}{S_o} \right)^{1.08} \left(\frac{g\mu_L^4}{\rho_L \sigma_L^3} \right)^{-0.0142}$$

$$\text{for} \quad 1 < \phi \leq 1.31 \quad (15)$$

where ϕ is the ratio of the right side of Eq. (14) and that of Eq. (15),

$$\phi = 0.178(1 - \varepsilon_a)^{-0.310} \left(\frac{\bar{U}_{Li}}{\sqrt{gD_i}} \right)^{0.310} \left(\frac{L}{D_i} \right)^{-0.319}$$

$$\times \left(\frac{S_a}{S_o} \right)^{-1.50} \left(\frac{S_i}{S_o} \right)^{-0.904} \left(\frac{g\mu_L^4}{\rho_L \sigma_L^3} \right)^{-0.0076} \quad (16)$$

The average errors of estimations of ΔP_l with Eqs. (13) and (14) and with Eqs. (13) and (15), respectively, were 13.5% for 68 data and 34.9% for 40 data. For the estimation of ΔP_l in columns of $(L/D_i) > 0.5$, it is recommended to estimate h_l with Eq. (14) or Eq. (15)

by assuming $(L/D_i)=0.5$.

Figure 7 shows that ΔP_l values estimated with the equation of Freedman et al.[6] agree relatively well with those observed in $10\,\mathrm{mol\cdot m^{-3}}$ KCl aq. soln and at $L/D_i=0.5$, but not with those observed in more viscous liquid or those observed in a column of $(L/D_i)<0.5$.

ΔP_u was calculated with Eq. (3) and the measured value of (P_3-P_2). **Figure 8** shows that ΔP_u is roughly equal to $\rho_L\{\bar{U}_{Li}/(1-\varepsilon_i)\}^2/2$ in the column of $(D_i/D_o)<0.6$. However, this relation does not hold if the value of D_i/D_o is increased further or if the clear liquid height is lowered to the level of the upper end of the draught tube, where ΔP_u increases drastically.

The liquid flow near the upper end of the draught tube was visualized by paths of tiny pieces of paper dispersed in liquid and entrained by the liquid flow. This observation shows that the liquid flow from the draught tube diverges to the space above the draught tube with change in its flow direction as shown in Fig. 1 and then converges into the annulus. Therefore, ΔP_u was assumed to be expressed in the form of loss of the divergence-convergence flow model where the effect of flow reversal on ΔP_u was considered on deciding numerical constants in the model equation with experimental data of ΔP_u.

$$\Delta P_u = 0.685\rho_L\left(\frac{\bar{U}_{Li}}{1-\varepsilon_i}\right)^2\left\{1-\frac{S_i(1-\varepsilon_i)}{S_o(1-\varepsilon_f)}\right\}^2$$
$$+0.945\rho_L\left(\frac{\bar{U}_{La}}{1-\varepsilon_a}\right)^2\left\{1-\frac{S_a(1-\varepsilon_a)}{S_o(1-\varepsilon_f)}\right\} \quad (17)$$

where ε_f is the gas holdup over the upper end of the draught tube,

$$\varepsilon_f = \{D_1^2\varepsilon_i+(D_o^2-D_1^2)\varepsilon_a\}/D_o^2 \quad (18)$$

The average error of estimating ΔP_u by Eq. (17) was 29.1% for 102 data.

3.2 Gas holdup in draught tube, ε_i

ε_i was found from Eq. (2) with data of (P_1-P_2) and τ_{wi} estimated from Takamatsu's result.[15]*1 **Figure 9** shows that ε_i increases with increasing gas velocity $\bar{U}_{Gi}$ in draught tube. As $\bar{U}_{Li}$ affects ε_i, the effect of column dimensions on ε_i is not clear from Fig. 9. However, when a single nozzle or a single orifice plate is used as a gas distributor, ε_i is lower than that for a perforated plate. Therefore, different correlations of ε_i with experimental conditions were tried for the perforated plate and for other gas distributors.

From the theoretical equations of Nicklin[13] for ε_i in finite liquid flow, Eq. (19) is derived.

$$(1/\varepsilon_i)-(1/\varepsilon_{i0})=(\bar{U}_{Li}/\bar{U}_{Gi}) \quad (19)$$

where ε_{i0} is gas holdup with no liquid flow. Since ε_i obtained for single nozzle and single orifice plate did
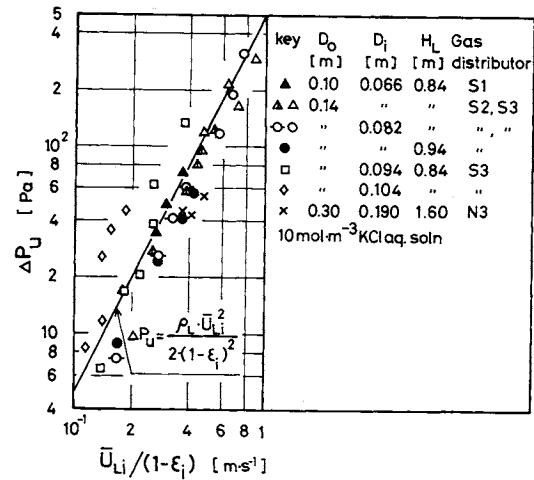
*1 See Appendix.

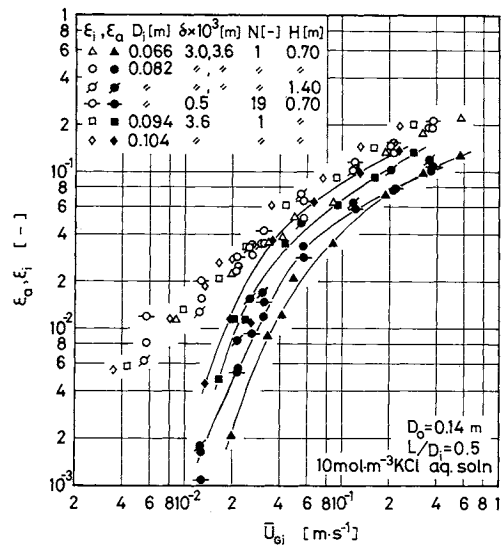**Fig. 8.** Effect of $\bar{U}_{Li}/(1-\varepsilon_i)$ on ΔP_u.

Fig. 9. Effect of $\bar{U}_{Gi}$ on gas holdup.

not agree with Eq. (19), $(1/\varepsilon_i-1/\varepsilon_{i0})$ was correlated with $\bar{U}_{Gi}$, $\bar{U}_{Li}$, D_i and the liquid properties by Eq. (20) with average error of 8.2% for 108 data, where ε_{i0} was estimated by the equation of Akita et al.[1]

$$\frac{1}{\varepsilon_i}-\frac{1}{\varepsilon_{i0}}=0.00894\left(\frac{\bar{U}_{Li}}{\bar{U}_{Gi}}\right)^{1.27}\left(\frac{\bar{U}_{Li}}{\sqrt{gD_i}}\right)^{-0.260}$$
$$\times\left(\frac{D_i^2 g\rho_L}{\sigma_L}\right)^{0.229}\left(\frac{g\mu_L^4}{\rho_L\sigma_L^3}\right)^{-0.101} \quad (20)$$

ε_i values observed for perforated plates were compared with those estimated by the method of Koide et al.,[9] and this showed that ε_i estimated agreed with values observed with average error of 10.3% for 18 data.

3.3 Gas holdup in annulus, ε_a

ε_a was found from Eq. (4) with measured value of (P_3-P_4) and τ_{wa} was assumed to be given by Eq. (21) for single-phase liquid flow.[5]

$$\tau_{wa}=0.085(D_e\bar{U}_{La}/\nu_L)^{-1/4}(\rho_L\bar{U}_{La}^2/2) \quad (21)$$

Figure 9 shows that ε_a increases with increasing $\bar{U}_{Gi}$, (D_i/D_o) and liquid viscosity. When the froth height H_f^{*2} from the upper end of the draught tube is decreased, many bubbles are entrained by the liquid flow before they reach top of the froth, and so ε_a increases. Based on these observations, the following empirical equation of ε_a was proposed. It correlates ε_a with experimental conditions with an average error of 28.1% for 97 data.

$$\frac{\varepsilon_a}{(1-\varepsilon_a)^4} = 26.3\varepsilon_i^{1.93}\left(\frac{\bar{U}_{La}}{\sqrt{gD_e}}\right)^{0.552}\left(\frac{S_o}{S_a}\right)^{1.25}$$
$$\times\left(\frac{S_a}{\pi D_1 H_f}\right)^{0.614}\left(\frac{H_L}{H}\right)^{0.814}\left(\frac{g\mu_L^4}{\rho_L\sigma_L^3}\right)^{0.0328}$$

(22)

Estimated values of ε_a by Eq. (22) agree relatively well with the experimental values of ε_a observed by Bohner et al.[4]

3.4 Flow rate of circulating liquid, Q_L

Figure 10 shows that Q_L in the 0.14 m dia. column increases with increasing $\bar{U}_G$ up to $\bar{U}_G \simeq 0.02\,\mathrm{m\cdot s^{-1}}$ but does not increase so much in the range of $\bar{U}_G > 0.02\,\mathrm{m\cdot s^{-1}}$. When D_i/D_o is kept constant, Q_L increases with increasing column diameter for a given gas velocity and also with increasing draught tube length, as the driving force of liquid circulation increases. When the liquid viscosity is higher, Q_L becomes smaller due to increasing value of ΔP_l. Figure 10 also shows that Q_L is larger when gas is dispersed by a perforated plate rather than a single orifice plate or a single nozzle. This might be due to the fact that the perforated plate generates smaller bubbles than the single nozzle or the single orifice plate and then ε_i becomes higher.

Figure 11 shows that the maximum value of Q_L is observed at $D_i/D_o \simeq 0.6$ for constant values of $\bar{U}_G$ and D_o. **Figure 12** shows that Q_L increases with increasing L in the range of $L/D_i \leqq 0.5$ but that further increase in L has almost no effect on Q_L. The reason is that ΔP_l decreases with increasing L in the range of $L/D_i \leqq 0.5$ but further increase in L has no effect on ΔP_l. The effect of the clear liquid height from the upper end of the draught tube on Q_L becomes small in the range of $(H_L - L - H)/D_i > 0.7$.

3.5 Estimation of Q_L and comparison with previous works

Q_L at a given gas velocity can be estimated by solving Eq. (6) or (9) numerically, as each term in Eqs. (6) and (9) is expressed as a function of Q_L, $\bar{U}_G$, the column dimensions, H_L and the liquid properties. ΔP_l, ΔP_u, ε_i, ε_a, τ_{wi} and τ_{wa} are expressed, respectively, by Eqs. (13), (17), (20), (22), (A1) and (21). Though most experiments were carried out in columns with a
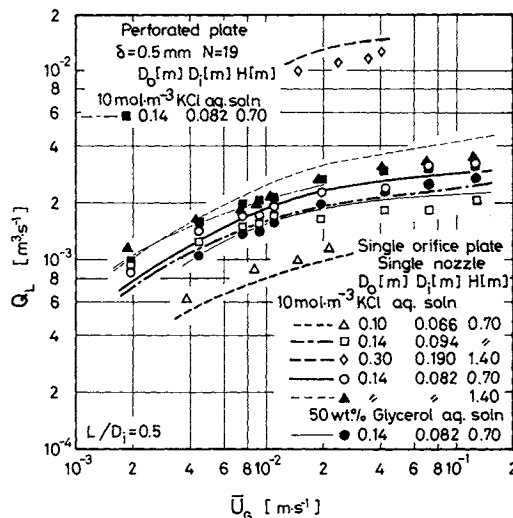
---

*2 Calculation of H_f is shown in Appendix.

Fig. 10. Effect of gas velocity, column diameter, draught tube length and liquid viscosity on Q_L (lines: values of Q_L estimated by Eq. (6)).
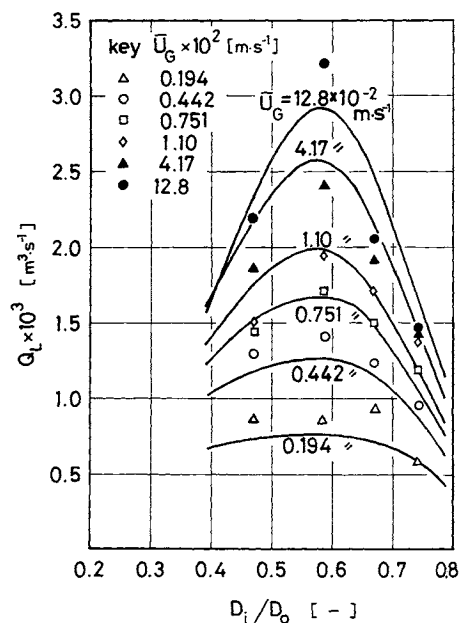

Fig. 11. Effect of D_i/D_o ratio on Q_L (Solid lines: Values of Q_L estimated by Eq. (6) for air–10 mol·m^{-3} KCl aq. soln system in column of $D_o=0.14$ m, $H=0.70$ m and $L/D_i=0.50$ m. Gas distributors: S2 for $U_G \leqq 0.11$ m·s^{-1} and S3 for $U_G > 0.11$ m·s^{-1}).
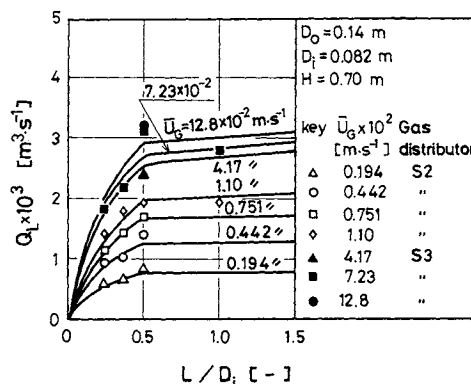
Fig. 12. Effect of L on Q_L (Solid lines: values of Q_L estimated by Eq. (6) for air–10 mol·m^{-3} KCl aq. soln system).

single orifice plate or a single nozzle as a gas distributor, the above method of estimating Q_L can be applied to the columns with a perforated plate if ε_i is estimated by the method of Koide et al.[9] instead of Eq. (20). Estimated values agree relatively well with those observed, as shown in Figs. 10–12, and the average error of estimating Q_L was 13% for 127 data.

The average velocity of circulating liquid $\bar{U}_{LC}$ defined by Eq. (1) was calculated from Q_L observed in the previous works[4,6,8] and in this work as shown in **Fig. 13**. $\bar{U}_{LC}$ observed by Bohner et al.[4] ($D_i/D_o = 0.572$ and $L/D_i = 0.439$) and Freedman et al.[6] ($D_i/D_o = 0.589$ and $L/D_i = 0.444$) roughly agreed with those observed in this work ($D_i/D_o \simeq 0.6$ and $L/D_i = 0.5$). $\bar{U}_{LC}$ values observed at different column diamters in this work agree well with each other if D_i/D_o and L/D_i are kept nearly constant. Figure 13 also shows that the values of $\bar{U}_{LC}$ estimated by the equation of Miyauchi et al.[12] for a bubble column without draught tube are much smaller than those in a column with draught tube. A rough estimation of the circulation time t_c ($= V_L/Q_L \simeq 2H_L/\bar{U}_{LC}$) can be made by using Fig. 13.

Figure 14 shows that ($\Delta P_l + \Delta P_u$) and ($\Delta P_{fa} + \Delta P_{fi}$) are about 70% and 30% of the total pressure drop, respectively, and ΔP_l is about 35–65% of the total pressure drop. Therefore, disregarding ΔP_{fa}, ΔP_{fi} and ΔP_u on estimating Q_L by Eq. (6), which was done by Freedman et al.,[6] results in an overestimate of Q_L value as Gopal et al.[8] have pointed out.

Conclusions

1) The flow rate of circulating liquid Q_L in a bubble column with draught tube increases with increasing gas velocity, column diameter, draught tube length and L/D_i ratio below 0.5 and decreases with increasing liquid viscosity. However, the maximum value of Q_L is observed at $D_i/D_o \simeq 0.6$ for constant values of gas velocity and column diameter.

2) Empirical equations of gas holdups in draught tube and annulus and the pressure drops due to flow reversals, necessary for estimating Q_L, are proposed.

Appendix

A.1 Evaluation of τ_{wi}

Koide et al.[10] derived Eq. (A1),

$$\tau_w = \tau_{w0}(k_L/k_{L0})^3 \tag{A1}$$

where k_L and τ_w are, respectively, the local mass transfer coefficient and the shear stress at the wall in gas-liquid two-phase flow. Takamatsu[15] proposed empirical equations for (k_L/k_{L0}) based on data found in a column of $D_i = 0.05$ m and air–20 mol·m^{-3} KCl aq. soln system and for the range of $\bar{U}_{Li} = 0.254$–0.511 m·s^{-1}: for perforated plate ($\delta = 1$ mm, $N = 19$),

$$(k_L/k_{L0}) = 1.08(\bar{U}_s/\bar{U}_{Li})^{1/2}, \qquad 0 < \varepsilon_i \leq 0.05 \tag{A2}$$

$$(k_L/k_{L0}) = 1.49\varepsilon^{1/8}(\bar{U}_s/\bar{U}_{Li})^{1/2}, \qquad 0.05 < \varepsilon_i \leq 0.15 \tag{A3}$$

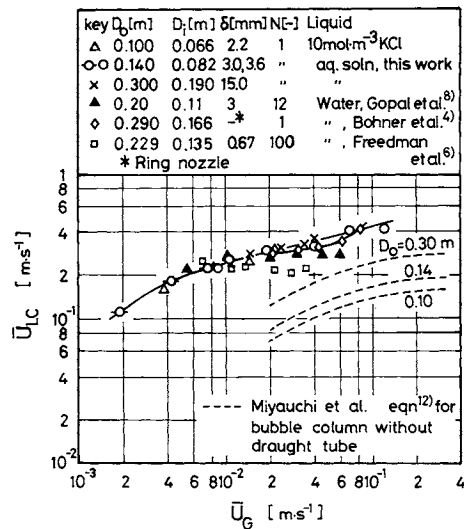and for single orifice plate ($\delta = 3$ mm, $N = 1$),

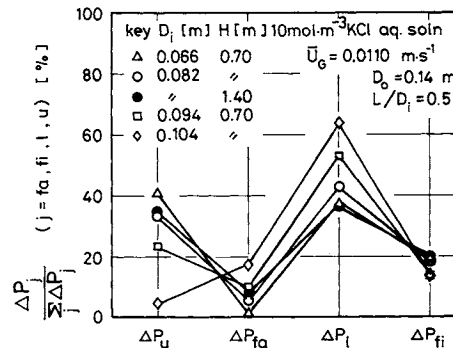**Fig. 13.** Comparison of average velocities of circulating liquid observed in this work with those in previous works.

Fig. 14. Comparison of pressure drops due to friction and flow reversal.

$$(k_L/k_{L0}) = 1.57\varepsilon^{1/11}(\bar{U}_s/\bar{U}_{Li})^{1/2}, \qquad 0 < \varepsilon_i \leq 0.15 \tag{A4}$$

τ_{wi} was evaluated with Eqs. (A1)–(A4), where τ_{w0} was calculated by using the Blasius friction factor.

A.2 Calculation of H_f

The liquid volume V_L and the gas volume V_G in the column are given by Eqs. (A5) and (A6), respectively.

$$V_L = S_o H_L - V_d \tag{A5}$$

$$V_G = S_o H_f \varepsilon_f + S_a H \varepsilon_a + S_i \varepsilon_i (H + L - H_N) \tag{A6}$$

Average gas holdup $\bar{\varepsilon}$ is given by Eq. (A7).

$$\bar{\varepsilon} = V_G/(V_G + V_L) \tag{A7}$$

The height H_f of the aerated liquid from the base plate is given by Eq. (A8).

$$H_F = (V_G + V_L + V_d)/S_o \tag{A8}$$

Referring to Fig. 1, H_f is given by Eq. (A9).

$$H_f = H_F - H - L \tag{A9}$$

Substituting Eqs. (A5), (A6) and (A8) into Eq. (A9) and rearranging it gives the following equation.

$$H_f = \frac{H_L - H - L}{1 - \varepsilon_f} + \frac{S_a H \varepsilon_a + S_i \varepsilon_i (H + L - H_N)}{S_o(1 - \varepsilon_f)} \tag{A10}$$

Acknowledgment

The authors wish to express their gratitude to Dr. Masuo Shindo for his useful suggestions. The authors are grateful to those undergraduate students at Shizuoka University who assisted in the experimental work.

Nomenclature

D	= inner diameter	[m]
D_e	= $(D_o - D_i - 2t_w)$	[m]
D_1	= $(D_i + t_w)$	[m]
g	= gravitational acceleration	[m·s^{-2}]
H	= length of draught tube	[m]
H_F, H_f	= level of aerated liquid, respectively, measured from base plate of column and from upper end of draught tube	[m]
H_L	= clear liquid height	[m]
H_N	= height of nozzle from base plate of column	[m]
h_l	= effective flow width of gas-liquid flow path shown in Fig. 1	[m]
i_d	= diffusion current	[A]
k_L	= local mass transfer coefficient at wall	[m·s^{-1}]
L	= distance between lower end of draught tube and base plate of column	[m]
N	= number of nozzles or pores	[—]
P_j	= static pressure at section j ($j = 1$–4)	[Pa]
$\Delta P_l, \Delta P_u$	= pressure drop due to flow reversal at lower end and at upper end of draught tube, respectively	[Pa]
ΔP_f	= frictional pressure drop	[Pa]
ΔP_t	= static pressure difference detected by pressure transducer	[Pa]
Q_G	= gas flow rate	[m^3·s^{-1}]
Q_L	= flow rate of circulating liquid	[m^3·s^{-1}]
S	= cross-sectional area	[m^2]
t_w	= wall thickness of draught tube	[m]
$\bar{U}_G, \bar{U}_{Gi}$	= gas velocity based on cross section of column and draught tube, respectively, and based on average static pressure in column	[m·s^{-1}]
$\bar{U}_L$	= average liquid velocity based on cross section	[m·s^{-1}]
U_{La}	= liquid velocity in annulus	[m·s^{-1}]
$\bar{U}_{LC}$	= average velocity of circulating liquid defined by Eq. (1)	[m·s^{-1}]
U_p	= probe velocity	[m·s^{-1}]
$\bar{U}_s$	= $\bar{U}_{Gi}/\varepsilon_i - \bar{U}_{Li}/(1 - \varepsilon_i)$	[m·s^{-1}]
V_d	= $H\pi\{D_i + 2t_w)^2 - D_i^2\}/4$, volume of draught tube	[m^3]
V_G, V_L	= volumes of gas and liquid, respectively	[m^3]

δ	= pore or nozzle diameter	[m]
ε	= gas holdup	[—]
ε_f	= gas holdup defined by Eq. (18)	[—]
ε_{i0}	= gas holdup in draught tube at $\bar{U}_{Li} = 0$	[—]
μ_L	= liquid viscosity	[Pa·s]
ν_L	= liquid kinematic viscosity	[m^2·s^{-1}]
σ_L	= liquid surface tension	[N·m^{-1}]
τ_w	= shear stress at wall	[Pa]

⟨Subscripts⟩

a	= annulus
est.	= estimated value
i	= draught tube
o	= column
obs.	= observed value
0	= single-phase liquid flow

Literature Cited

1) Akita, K. and F. Yoshida: *Ind. Eng. Chem., Process Des. Develop.*, **12**, 76 (1973).
2) Blenke, H.: *Advan. Biochem. Eng.*, **13**, 121 (1979).
3) Blenke, H., K. Bohner and W. Hirner: *Verfahrenstechnik*, **3**, 444 (1969).
4) Bohner, K. and H. Blenke: *Verfahrenstechnik*, **6**, 50 (1972).
5) Brighton, J. A. and J. B. Johnes: *J. Bas. Eng. Trans. ASME*, **86**, 835 (1964).
6) Freedman, W. and J. F. Davidson: *Trans. Inst. Chem. Eng.*, **47**, T-251 (1969).
7) Fujie, K. and H. Kubota: *Suishitsu Odaku Kenkyu*, **3**, 15 (1980).
8) Gopal, J. S. and M. M. Sharma: *Can. J. Chem. Eng.*, **60**, 353 (1982).
9) Koide, K., T. Hirahara and H. Kubota: *Kagaku Kōgaku*, **30**, 712 (1966).
10) Koide, K. and H. Kubota: *Kagaku Kōgaku*, **30**, 801 (1966).
11) Kubota, H., Y. Hosono and K. Fujie: *J. Chem. Eng., Japan*, **11**, 319 (1978).
12) Miyauchi, T., S. Furusaki, S. Morooka and Y. Ikeda: *Adv. Chem. Eng.*, **11**, 275 (1981).
13) Nicklin, D. J.: *Chem. Eng. Sci.*, **17**, 693 (1962).
14) Reiss, L. P. and T. J. Hanratty: *AIChE J.*, **9**, 154 (1963).
15) Takamatsu, T.: Master Thesis, Tokyo Institute of Technology (1969).